A new method for the reconstruction of unknown non-monotonic growth functions in the chemostat

Jan Sieber*, Alain Rapaport†, Serafim Rodrigues‡and Mathieu Desroches§

May 14, 2012

Abstract

We propose an adaptive control law that allows one to identify unstable steady states of the open-loop system in the single-species chemostat model without the knowledge of the growth function. We then show how to use a continuation method to reconstruct the whole graph of the growth function. Two variants, in continuous and discrete time, are presented. The case of two species in competition is also examined.

1 Introduction

We recall the classical chemostat model [19] for a single species (biomass b) consuming a substrate (mass s):

$$\left\{ \begin{array}{rcl} \dot{s} & = & -\mu(s)b + D(s_{in} - s) \\ \dot{b} & = & \mu(s)b - Db \end{array} \right. \tag{1}$$

where the *dilution rate* D (the *input*) is the manipulated variable, which takes values in a bounded positive interval $[D_{\min}, D_{\max}]$, and $\mu(\cdot)$ is a non-negative Lipschitz continuous function with $\mu(0) = 0$.

We consider here the following scenario: the function $\mu(\cdot)$ is unknown and possibly non-monotonic. Our objective is to reconstruct the graph of the function $\mu(\cdot)$ on the domain $(0, s_{in})$ by varying the input D in time. On-line measurements are only available for the variable s (that is, s is the *output*). This setup is realistic for experimental investigations such as in [3], however, demonstrations in this paper are based entirely on simulations of model system (1).

Remark: We assume that the yield coefficient of the bio-conversion is known. Then we can choose it equal to unity without loss of generality such that $\mu(s)b$ appears with the same pre-factor 1 (once positive, and once negative) in both equations of (1)).

The problem of kinetics estimation in biological and biochemical models has been widely addressed in the literature ([9, 10, 11, 4, 12, 16, 8]), either as a parameter estimation problem (one chooses a priori analytical expression of the function $\mu(\cdot)$), or as an on-line estimation of the kinetics (one aims at determining $\mu(s(t))$ at the current time t). Here, our objective is different: we aim at reconstructing the whole graph of the function $\mu(\cdot)$. To our knowledge, this precise problem has not been addressed in the literature.

When the growth function is monotonic, a common way to reconstruct points on the graph of the growth function $\mu(\cdot)$ is to design a series of experiments fixing the dilution rate D with different values and wait

*J. Sieber is with CEMPS, Univ. of Exeter, U.K. E-mail: J.Sieber@exeter.ac.uk

†A. Rapaport is with UMR INRA/SupAgro MISTEA and EPI INRA/INRIA MODEMIC, Montpellier, France. E-mail: rapaport@supagro.inra.fr *(corresponding author)*

‡S. Rodrigues is with CN-CR, Univ. of Plymouth, U.K. E-mail: serafim.rodrigues@plymouth.ac.uk

§M. Desroches is with EPI SISYPHE, INRIA Rocquencourt, France. E-mail: Mathieu.Desroches@inria.fr

until the system settles to a steady state $(s^\star, b^\star)$ [4]. As long as D is less than $\mu(s_{in})$, it is well known that the dynamics converges to a unique positive equilibrium that satisfies $\mu(s^\star) = D$ (see for instance [19]). An alternative approach is to fix a value of s, say $\bar{s}$ and design an adaptive control law $D(\cdot)$ that stabilizes the system about the steady state $(\bar{s}, s_{in} - \bar{s})$, with the value of D converging to $\mu(\bar{s})$. This technique has been proposed in [3] to stabilize such dynamics without the knowledge of $\mu(\cdot)$ and under the constraint $D \in [D_{\min}, D_{\max}]$.

Unfortunately, these two reconstruction strategies cannot be used to identify non-monotonic growth functions, such as the Haldane law. More precisely, these two techniques require the steady state to be stable in open loop, and consequently cannot reconstruct any part of the graph of a function $\mu(\cdot)$ where μ is non-increasing (such as the example, shown schematically in Figure 1. Furthermore, the global convergence of these methods is not satisfied in case of bi-stability, which is present in (1), with non-monotonic growth functions μ (see again [19]).

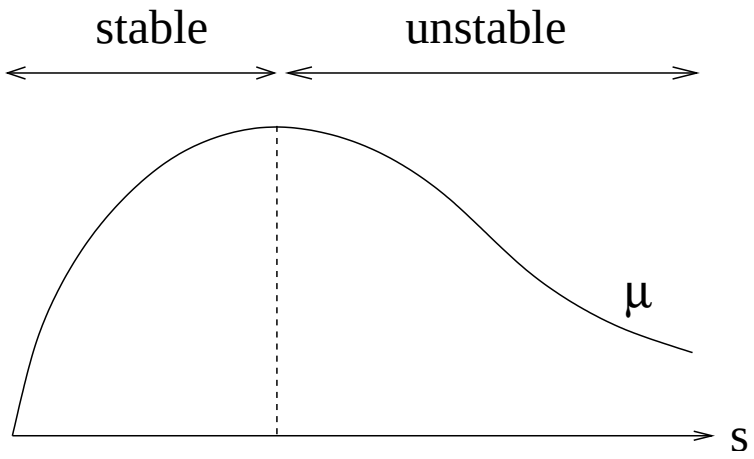

Figure 1: Domains of stability and instability in open-loop

In this work, we first propose that it can be useful to introduce a feedback control loop into (1) to identify the growth function μ of the *open-loop* system (1) (that is, (1) with constant input D). The feedback control law is initially a simple constrained piecewise linear relation between system input D and system output s:

$$D(s, \bar{D}, \bar{s}) = \mathrm{sat}_{[D_{\min}, D_{\max}]} \left(\bar{D} - G_1(s - \bar{s}) \right), \tag{2}$$

where $\bar{D}$ and $\bar{s}$ are reference values, and $G_1 > 0$ is the linear control gain. To ensure realistic values for the input D, we enclose the feedback rule into the saturation function

$$\mathrm{sat}_{[D_{\min}, D_{\max}]}(x) = \begin{cases} D_{\max} & \text{if } x > D_{\max}, \\ x & \text{if } x \in [D_{\min}, D_{\max}], \\ D_{\min} & \text{if } x < D_{\min}, \end{cases}$$

where the limits $D_{\min}$ and $D_{\max}$ are the extreme dilution rates that can be achieved experimentally. In sections 3 and 5 we will then explore adaptation rules for the reference values $(\bar{s}, \bar{D})$ which ensure that asymptotically for $t \to \infty$ the input satisfies

$$D(s, \bar{D}, \bar{s}) = \bar{D}, \tag{3}$$

or, equivalently, the output satisfies

$$s = \bar{s}, \tag{4}$$

such that the control is asymptotically *non-invasive*. The result is a new adaptive control law that stabilizes the dynamics about any desired equilibrium point without requiring a-priori knowledge of its location, and whatever is the monotonicity of the growth function. One requirement on the adaptive law is that it should work uniformly well around a local maximum of μ (non-invasive feedback laws such as filtered feedback [1] or time-delayed feedback [17] do not achieve this).

We propose two variants of our method, making adaptation in continuous time (Section 3) or in discrete time (Section 5).

Then we show that a simple continuation method allows us to the reconstruct continuously the graph of the growth function, even in the case of non-monotonic growth functions. Finally we investigate the case of two species that compete for the same common substrate.

2 Global stability of the simple feedback law

Our starting point is that the feedback law (2) is, within reasonable limits, globally stabilizing. Suppose that we choose the reference value $\bar{s}$ from an interval $[s_{\min}, s_{\text{in}}) \subset (0, s_{\text{in}})$, and that the limits on the input cover the growth function μ on this interval:

$$D_{\min} < \mu(s) \quad \text{for all } s \in [s_{\min}, s_{\text{in}}], \tag{5}$$

$$D_{\max} > \mu(s) \quad \text{for all } s \in [0, s_{\text{in}}]. \tag{6}$$

These conditions mean that the graph of μ does not cross the thick parts of the horizontal lines $D_{\min}$ and $D_{\max}$ bounding the grey area in Figure 2 from below and above.

Proposition 1. Suppose that the reference values $(\bar{s}, \bar{D})$ are chosen from $[s_{\min}, s_{\text{in}}) \times [D_{\min}, D_{\max}]$, that the growth function μ satisfies (5)–(6), and that the gain G_1 is chosen sufficiently large, that is,

$$G_1 > -\min_{s \in [0, s_{\text{in}}]} \mu'(s), \text{ and} \tag{7}$$

$$G_1 > \frac{\mu(s_{\text{in}}) - \bar{D}}{s_{\text{in}} - \bar{s}}. \tag{8}$$

Then the controlled system (1) with $D = D(s, \bar{D}, \bar{s})$, given in (2), has a stable equilibrium $(s_{\text{eq}}, b_{\text{eq}}) \in [0, s_{\text{in}}) \times (0, \infty)$, which attracts all initial conditions $(s(0), b(0)) \in [0, s_{\text{in}}) \times (0, \infty)$.

Proof of Proposition 1. If $D > 0$, and the growth function μ satisfies $\mu(0) = 0$ and, for $s > 0$, $\mu(s) > 0$ then the set

$$R = \{(s, b) : s \in [0, s_{\text{in}}), b > 0\}$$

is positively invariant (that is, trajectories starting in R will stay in R for all positive times). Furthermore, all trajectories starting in R approach the subspace

$$T = \{(s, b) \in R : s + b = s_{\text{in}}\}$$

with rate at least $D_{\min}$ forward in time. This implies that it is sufficient to check if all trajectories in T converge to a unique equilibrium. On T the equation of motion can be expressed as a differential equation for s only:

$$\dot{s} = [D(s, \bar{D}, \bar{s}) - \mu(s)][s_{\text{in}} - s]. \tag{9}$$

First, let us check that the equilibrium at $s = s_{\text{in}}$ is unstable. The term $-G_1(s_{\text{in}} - \bar{s})$ is negative such that $\bar{D} - G_1(s_{\text{in}} - \bar{s}) < D_{\max}$ for all admissible $\bar{D}$. Assumption (8) guarantees that $\bar{D} - G_1(s_{\text{in}} - \bar{s}) < \mu(s_{\text{in}})$. Assumption (5) guarantees that also $D_{\min} < \mu(s_{\text{in}})$. Hence,

$$D(s_{\text{in}}, \bar{D}, \bar{s}) - \mu(s_{\text{in}}) < 0$$

for all admissible $(\bar{s}, \bar{D})$. Thus, the prefactor of $s_{\text{in}} - s$ in (9) is negative such that the equilibrium at s_{in} is unstable for all admissible $(\bar{s}, \bar{D})$.

Since $\dot{s} > 0$ at $s = 0$, there must be other equilibria of (9) in $(0, s_{\text{in}})$, which are given as solutions s_{eq} of $D(s_{\text{eq}}, \bar{D}, \bar{s}) = \mu(s_{\text{eq}})$. Now let us check indirectly that none of the equilibria can satisfy $D_{\min} = \mu(s_{\text{eq}})$.

Assume that (9) had an equilibrium s_{eq} with $D_{\min} = \mu(s_{\text{eq}})$. Then s_{eq} has to be less than $s_{\min}$ due to assumption (5). However, if $s_{\text{eq}} < s_{\min}$, then $\bar{D} - G_1(s_{\text{eq}} - \bar{s}) > \bar{D} \geq D_{\min}$ for all admissible $(\bar{s}, \bar{D})$. Hence $D(s_{\text{eq}}, \bar{D}, \bar{s}) > D_{\min}$ (recall that $D_{\min} = \mu(s_{\text{eq}})$ by assumption of the indirect proof) such that $D(s_{\text{eq}}, \bar{D}, \bar{s}) - \mu(s_{\text{eq}}) > 0$, which means that s_{eq} cannot be equilibrium.

Assumption (6) excludes that equilibria with $\mu(s_{\text{eq}}) = D_{\max}$ exist, hence all remaining equilibria $s_{\text{eq}} \in (0, s_{\text{in}})$ must satisfy

$$\bar{D} - G_1(s_{\text{eq}} - \bar{s}) = \mu(s_{\text{eq}}).$$

Condition (7) ensures that this equation has a unique solution and that this solution corresponds to a stable equilibrium (which must be in $(0, s_{\text{in}})$ because the boundaries of $(0, s_{\text{in}})$ are inflowing for (9)). □

Proposition 1 ensures that the output s_{eq} of the controlled system (1) with (2), after transients have decayed, is a well-defined smooth function of the parameters $(\bar{s}, \bar{D})$ as long as $(\bar{s}, \bar{D})$ are chosen from $(s_{\min}, s_{\max}) \times (D_{\min}, D_{\max})$. We express this fact by using the bracket notation:

$$s_{\text{eq}}(\bar{s}, \bar{D}) = \lim_{t \to \infty} s(t) \quad \text{where } s \text{ is output of } (1), (2).$$

The function s_{eq} can be evaluated at any admissible point by setting the parameters $(\bar{s}, \bar{D})$ in the definition (2) of the feedback rule, waiting until the transients of (1) have settled, and then reading off the output s. Equilibria of the uncontrolled system can then, according to (4), be found as roots of $s_{\text{eq}}(\bar{s}, \bar{D}) - \bar{s}$. More specifically, we know that, for any admissible $\bar{s}$,

$$\bar{D} = \mu(\bar{s}) \quad \text{if and only if } s_{\text{eq}}(\bar{s}, \bar{D}) = \bar{s}. \tag{10}$$

Relation (10) permits us to identify $\mu(\bar{s})$ as the unique root of $s_{\text{eq}}(\bar{s}, \cdot) - \bar{s}$. Sections 3-5 will explore two strategies to find this root for a range of admissible $\bar{s}$ efficiently.

3 An adaptive control scheme

The first strategy is a dynamic feedback that comes on top of the feedback law (2) for D. We treat $\bar{D}$ not as a parameter but introduce an additional dynamical equation for $\bar{D}$, achieving local convergence of the output s to any reference value $\bar{s} \in (0, s_{in})$ without the knowledge of the growth function μ. The asymptotic value of $\bar{D}$ allows then one to reconstruct the value $\mu(\bar{s})$.

Proposition 2. Fix a number $\bar{s} \in (0, s_{\text{in}})$ and take numbers $D_{\min}$, $D_{\max}$ that fulfill $0 < D_{\min} < \mu(\bar{s}) < D_{\max}$. Then the dynamical feedback law

$$\begin{aligned} D(s, \bar{D}) &= \text{sat}_{[D_{\min}, D_{\max}]} \left(\bar{D} - G_1(s - \bar{s}) \right) \\ \dot{\bar{D}} &= -G_2(s - \bar{s})(\bar{D} - D_{\min})(D_{\max} - \bar{D}) \end{aligned} \tag{11}$$

exponentially stabilizes the system (1) locally about $(s, b) = (\bar{s}, s_{\text{in}} - \bar{s})$, for any positive constants (G_1, G_2) such that $G_1 > -\mu'(\bar{s})$. Furthermore one has

$$\lim_{t \to +\infty} \bar{D}(t) = \mu(\bar{s})$$

Note that the assumptions in Proposition 2 (for example, on the gain G_1) are weaker than those of Proposition 1 as Proposition 2 is only concerned with local stability and a single reference value $\bar{s}$.

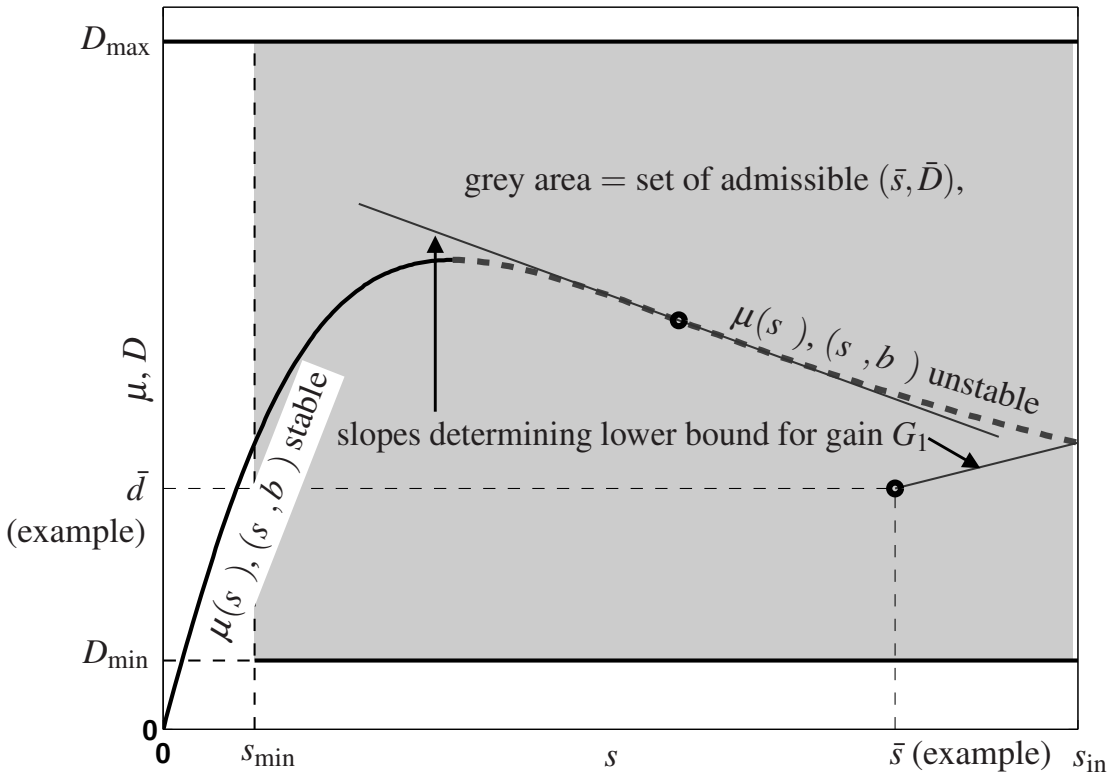

Figure 2: Sketch illustrating shape of growth function μ and set of admissible reference values

Proof of Proposition 2. Locally about $s = \bar{s}$, the closed loop system is equivalent to the three-dimensional dynamical system

$$\left\{ \begin{array}{rcl} \dot{s} & = & -\mu(s)b + (\bar{D} - G_1(s-\bar{s}))(s_{\text{in}} - s) \\ \dot{b} & = & \mu(s)b - (\bar{D} - G_1(s-\bar{s}))b \\ \dot{\bar{D}} & = & -G_2(s-\bar{s})(\bar{D} - D_{\min})(D_{\max} - \bar{D}) \end{array} \right.$$

This system admits the unique positive equilibrium $E^{\star} = (\bar{s}, s_{\text{in}} - \bar{s}, \mu(\bar{s}))$.
For simplicity, we write the dynamics in the variables $(z, s, \bar{D})$ coordinates, where z is defined as $z = s + b$:

$$\left\{ \begin{array}{rcl} \dot{z} & = & (\bar{D} - G_1(s-\bar{s}))(s_{\text{in}} - z) \\ \dot{s} & = & -\mu(s)(z-s) + (\bar{D} - G_1(s-\bar{s}))(s_{\text{in}} - s) \\ \dot{\bar{D}} & = & -G_2(s-\bar{s})(\bar{D} - D_{\min})(D_{\max} - \bar{D}) \end{array} \right.$$

The Jacobian matrix at $E^{\star}$ in these coordinates is

$$\left(\begin{array}{ccc} -\mu(\bar{s}) & 0 & 0 \\ -\mu(\bar{s}) & -(\mu'(\bar{s}) + G_1)(s_{\text{in}} - \bar{s}) & s_{\text{in}} - \bar{s} \\ 0 & -G_2(\mu(\bar{s}) - D_{\min})(D_{\max} - \mu(\bar{s})) & 0 \end{array} \right)$$

Its eigenvalues are $\lambda_1 = -\mu(\bar{s}) < 0$ and λ_2, λ_3 as eigenvalues of the sub-matrix

$$M = \left(\begin{array}{cc} -(\mu'(\bar{s}) + G_1)(s_{\text{in}} - \bar{s}) & s_{\text{in}} - \bar{s} \\ -G_2(\mu(\bar{s}) - D_{\min})(D_{\max} - \mu(\bar{s})) & 0 \end{array} \right)$$

Then, one has

$$\begin{array}{rcl} \det(M) & = & G_2(\mu(\bar{s}) - D_{\min})(D_{\max} - \mu(\bar{s}))(s_{\text{in}} - \bar{s}) \\ \text{tr}(M) & = & -(\mu'(\bar{s}) + G_1)(s_{\text{in}} - \bar{s}) \end{array}$$

and concludes about the exponential stability of $E^\star$ when $G_2 > 0$ and $G_1 > -\mu'(\bar{s})$. Finally, one obtains from (11) that D or $\bar{D}$ converges toward the unknown value $\mu(\bar{s})$. □

4 Reconstruction of the entire growth function

Now, we use a dynamic continuation method, letting $\bar{s}$ change slowly with time as solution of the simple dynamics

$$\dot{\bar{s}} = \varepsilon \bar{s}(s_{\text{in}} - \bar{s}) \tag{12}$$

to explore the right part of the graph of $\mu(\cdot)$ when ε is a small non-negative number, and to explore the left one when ε is a small non-positive number. Recall that continuation denotes a numerical method that belongs to the family of homotopy methods and is used to compute solution branches of parametrized nonlinear equations via a predictor-corrector strategy [2]. For the continuation, the gain G_1 has to be been chosen uniformly large according to (7).

5 A discrete-time adaptation of the method

In this section, we propose an alternative to the continuous adaptation of $\bar{D}$ and $\bar{s}$: we treat the root problem $0 = s_{\text{eq}}(\bar{s}, \bar{D}) - \bar{s}$ with ordinary numerical root-finders such as the Newton iteration. We present here an approach that combines the two steps of the method (the adaptive control and the continuation) in a discrete time framework.

In an experimental setting one will have to adapt the numerical methods to the lower accuracy of experimental outputs (see [18] for a demonstration in a mechanical experiment) but for this paper we restrict ourselves to a numerical demonstration. In the single-species case, one profits from the knowledge of an approximate derivative of s_{eq} with respect to $\bar{D}$ to make the Newton iteration more efficient. Suppose, we plan to identify the growth function μ in a sequence of points $\bar{s}_k = \bar{s}_0 + k\delta$ (where $\delta > 0$ is small). The function values $\mu(\bar{s}_k)$ are the roots $\bar{D}_k$ of $s_{\text{eq}}(\bar{s}_k, \cdot) - \bar{s}_k$. Then we can approximate

$$\frac{\partial s_{\text{eq}}}{\partial \bar{D}}(\bar{D}, \bar{s}_k) = \frac{1}{G_1 + \mu'(s_{\text{eq}}(\bar{D}, \bar{s}_k))} \approx \frac{1}{G_1 + \frac{\bar{D} - \bar{D}_{k-1}}{\bar{s}_k - \bar{s}_{k-1}}}$$

to obtain the iteration

$$\bar{D}_{\text{new}} = \bar{D} - \frac{s_{\text{eq}}(\bar{D}, \bar{s}_k)}{G_1 + \frac{\bar{D} - \bar{D}_{k-1}}{\bar{s}_k - \bar{s}_{k-1}}}, \tag{13}$$

starting from $\bar{D} = \bar{D}_{k-1}$, or (for $k > 2$)

$$\bar{D} = \bar{D}_{k-1} + \frac{\bar{D}_{k-1} - \bar{D}_{k-2}}{\bar{s}_{k-1} - \bar{s}_{k-2}}.$$

For the initial step ($k = 1$) the derivative of s_{eq} has to be either guessed or approximated with a finite difference (we used the latter in our numerical simulations).

Note that at no point it is necessary to set the internal states s or b of system (1). Only the reference values $(\bar{s}, \bar{D})$ have to be set.

5.1 A simplified discrete scheme

The scheme (13) permits one to find $\mu(\bar{s}_k)$ for an a-priori prescribed set of admissible abscissae $\bar{s}_k$. If one wants to recover only the graph of μ one does not need to prescribe the sequence $\bar{s}_k$ a-priori, thus, avoiding a Newton iteration. Suppose that we know already two points $p_{k-1} = (s_{k-1}, D_{k-1})$ and $p_k = (s_k, D_k)$ on the curve $(s, \mu(s))$. Then we set

$$(\bar{s}_{\text{new},k+1}, \bar{D}_{\text{new},k+1}) = p_k + \delta \frac{p_k - p_{k-1}}{\|p_k - p_{k-1}\|}, \tag{14}$$

where $\delta > 0$ is the approximate desired distance between points along the curve $(s, \mu(s))$, and run the controlled experiment with the reference values $(\bar{s}, \bar{D}) = (\bar{s}_{\text{new},k+1}, \bar{D}_{\text{new},k+1})$ in (2) until the transients have settled to obtain the next point on the curve

$$\begin{aligned} s_{k+1} &= s_{\text{eq}}(\bar{s}_{\text{new},k+1}, \bar{D}_{\text{new},k+1}) \\ D_{k+1} &= D(s_{k+1}, \bar{D}_{\text{new},k+1}, \bar{s}_{\text{new},k+1}) \\ &= \bar{D}_{\text{new},k+1} - G_1(s_{k+1} - \bar{s}_{\text{new},k+1}) \end{aligned} \tag{15}$$

This simplified procedure cannot guarantee the identification of μ at prescribed equidistantly spaced values of s but finds $\mu(s_k)$ for a (nearly evenly spaced) sequence s_k given by the intersections of the lines $D = D_{\text{new},k} - G_1(s - \bar{s}_{\text{new},k})$ with the graph $D = \mu(s)$.

6 The two species case

The extension of the chemostat model (1) considers two species that compete for the same substrate. The two-species model can be written as follows

$$\left\{ \begin{array}{rcl} \dot{s} &=& -\displaystyle\sum_{i=1}^{2} \mu_i(s) b_i + D(s_{\text{in}} - s) \\ \dot{b}_i &=& \mu_i(s) b_i - D b_i \qquad (i = 1, 2) \end{array} \right. \tag{16}$$

The two-species model has co-existing equilibria E_i^*, which correspond to the state where species i is present but the other species is not. The following result shows that feedback stabilization based on input D and output s breaks down for the equilibrium corresponding to the species with the smaller growth rate.

Proposition 3. Fix $\bar{s} \in (0, s_{\text{in}})$ and consider the equilibrium $E_2^\star = (\bar{s}, 0, s_{\text{in}} - \bar{s})$.

1. If $\mu_1(\bar{s}) > \mu_2(\bar{s})$, there does not exist feedback $D(\cdot)$ of the form

   $$D = f(s, \xi), \quad \dot{\xi} = g(s, \xi), \qquad (\xi \in \mathbb{R}^k)$$

   with $f(\bar{s}, 0) = \mu_2(\bar{s})$ and $g(\bar{s}, 0) = 0$, that stabilizes asymptotically the system (16) about $E_2^\star$.

2. If $\mu_1(\bar{s}) < \mu_2(\bar{s})$, then the feedback (11) exponentially stabilizes the system (16) locally about $E_2^\star$, for any positive constants (G_1, G_2) such that $G_1 > -\mu_2'(\bar{s})$. Furthermore one has

   $$\lim_{t \to +\infty} \bar{D}(t) = \mu_2(\bar{s})$$

Proof of Proposition 3. Consider the extended dynamics

$$\left\{ \begin{array}{rcl} \dot{s} &=& -\displaystyle\sum_{i=1}^{2} \mu_i(s) b_i + f(s, \xi)(s_{\text{in}} - s) \\ \dot{b}_i &=& \mu_i(s) b_i - f(s, \xi) b_i \qquad (i = 1, 2) \\ \dot{\xi} &=& g(s, \xi) \end{array} \right.$$

that we write in (z, b_1, b_2, ξ) coordinates with $z = s + b_1 + b_2$:

$$\left\{ \begin{array}{rcl} \dot{z} &=& f(z - b_1 - b_2, \xi)(s_{\text{in}} - z) \\ \dot{b}_i &=& (\mu_i(z - b_1 - b_2) - f(z - b_1 - b_2, \xi)) b_i \\ \dot{\xi} &=& g(z - b_1 - b_2, \xi) \end{array} \right.$$

1. At equilibrium $E_2^\star$, the Jacobian matrix possesses the following form in (z, b_1, b_2, ξ) coordinates

$$\begin{pmatrix} -\mu_2(\bar{s}) & 0 & 0 & 0 \\ 0 & \mu_1(\bar{s}) - \mu_2(\bar{s}) & 0 & 0 \\ \star & \star & \star & \star \\ \star & \star & \star & \star \end{pmatrix},$$

which has the positive eigenvalue $\mu_1(\bar{s}) - \mu_2(\bar{s})$. This proves that E_2^* is unstable whatever the choice of the feedback $D(\cdot)$.

2. At equilibrium $E_2^\star$, the Jacobian matrix can be written as follows, in $(z, b_1, b_2, \bar{D})$ coordinates

$$\begin{pmatrix} -\mu_2(\bar{s}) & 0 & \\ 0 & \mu_1(\bar{s}) - \mu_2(\bar{s}) & 0 \\ & \star & \mathrm{M} \end{pmatrix}$$

with

$$M = \begin{pmatrix} -(\mu_2'(\bar{s}) + G_1)(s_{\mathrm{in}} - \bar{s}) & s_{\mathrm{in}} - \bar{s} \\ -G_2(\mu_2(\bar{s}) - D_{\min})(D_{\max} - \mu_2(\bar{s})) & 0 \end{pmatrix}$$

Its eigenvalues are $\lambda_1 = -\mu_2(\bar{s}) < 0$, $\lambda_2 = \mu_1(\bar{s}) - \mu_2(\bar{s}) < 0$, λ_3 and λ_4 with

$$\begin{array}{lcl} \lambda_3.\lambda_4 & = & G_2(\mu_2(\bar{s}) - D_{\min})(D_{\max} - \mu_2(\bar{s}))(s_{\mathrm{in}} - \bar{s}) \\ \lambda_3 + \lambda_4 & = & -(\mu_2'(\bar{s}) + G_1)(s_{\mathrm{in}} - \bar{s}) \end{array}$$

As in the proof of Proposition 2, one concludes the exponential stability of $E_2^\star$ when $G_2 > 0$ and $G_1 > -\mu_2'(\bar{s})$, and the convergence of $D(\cdot)$ toward $\mu_2(\bar{s})$. □

Consequently, the adaptive control scheme proposed in Section 3 only allows one to reconstruct the larger of the two growth rates at any given s. Nevertheless, the dynamics of (12), which defines the dynamic continuation method presented in Section 4, may still be of help in reconstructing the smaller growth rate at least in some cases. Suppose that the graphs μ_1 and μ_2 cross each other at some value s_c, say, $\mu_1(s) < \mu_2(s)$ for $s < s_c$ but $\mu_1(s) > \mu_2(s)$ for $s > s_c$. If one treats $\bar{s}$ as a parameter then the equilibria E_1^* and E_2^* undergo an exchange of stability (a degenerate transcritical bifurcation) at $\bar{s} = s_c$. As the continuation rule (12) lets $\bar{s}$ drift slowly (with speed ε) the full system exhibits a phenomenon known as delayed loss of stability [6] in the context of dynamic bifurcations [5], widely studied in slow-fast systems. Physically this means (say, we are increasing $\bar{s}$ slowly from below s_c) that concentration b_2 comes close to 0 while $\bar{s} < s_c$. Then, when $\bar{s}$ has crossed s_c, the concentration b_2 grows exponentially, but still takes some time until it reaches values noticeably different from 0. The value $\bar{s}_{\mathrm{loss}}$ of $\bar{s}$ at which b_2 becomes noticeably non-zero is in the ideal ODE model independent of the drift speed ε of $\bar{s}$. Figure 7 in Section 7 shows this effect: since b_2 is nearly zero the variable D continues to follow the, by now unstable, drifting equilibrium E_1^*. This delay mechanism allows one in principle a reconstruction of a part of the slower growth rate close to the about the bifurcation value of $\bar{s}$. This is in line with the philosophy behind continuation methods, which allow one to track both stable and unstable solution branches, hence, to go past bifurcation points.

The numerical simulations show only the case of continuously drifting $\bar{s}$. Setting the value of $\bar{s}$ at discrete times (as one would do in the discrete-time framework of Section 5), achieves the same delay effect.

7 Numerical simulations

Figures are given at the end of the paper.

7.1 The one species case

For the unknown function, we have chosen the non-monotonic Haldane function

$$\mu(s) = \frac{s}{1 + s + 10s^2}$$

and $s_{\text{in}} = 1$. The grey background curve in Figure 3 shows $\mu(\cdot)$, which is clearly non-monotonic on the domain $(0, s_{\text{in}})$ ($s_{\text{in}} = 1$). Figure 3 shows the stabilization of the control law (11) for $\bar{s}$ in the increasing (left panel) and decreasing (right panel) part of the growth law μ. Figure 4 shows how the continuation (12) reconstructs the entire graph of the growth function. For the left panel, $\varepsilon = +0.01$, and for the right panel, $\varepsilon = -0.01$.

Figure 5 shows the output of a simulation with the discrete-time adaptation method proposed in Section 5. The black dots correspond to values at which the control was accepted as non-invasive. Using continuation one achieves small and rapidly decaying transients in every evaluation of s_{eq} (which involves running system (1) with control until transients have settled). This is so because the transients all lie inside the subspace $\{(s, b) : s + b = s_{\text{in}}\}$ after system (1) has run at least once. Second, the initial offset from the equilibrium is always small, because the adjustments of $\bar{s}$ and $\bar{D}$ are small.

Figure 6 demonstrates the speed-up using the simplified scheme (14)–(15) (note the times at the abscissae). The difference to Figure 5 is that the values at which the growth function is evaluated are not exactly equidistantly spaced.

7.2 The two species case

We have chosen two monotonic Monod functions

$$\mu_1(s) = \frac{s}{0.1 + s}, \qquad \mu_2(s) = 1.5\frac{s}{0.4 + s}$$

and $s_{\text{in}} = 1$. Their graphs are shown as faint curves in the background of Figure 7. The simulations depicted in Figure 7 have been made with the drift speed parameter ε equal to ± 0.01. One can see that the delayed loss of stability permits us to reconstruct parts of the graphs of the growth curves that do not belong to their supremum envelope.

From a practical view point, the sudden "jump" between the two graphs could inform of the presence of another species, if one belongs that the culture in chemostate was initially pure.

Remark. If the drift speed ε of the continuation is too small the concentration of the initially suppressed species (for example, b_2 in the left panel of Figure 7) will become unrealistically small in the numerical simulations. In a real experiment this would correspond to the species becoming almost extinct. This makes the validity of the ODE model (16) with two species questionable as a good representation of reality [7] such that it is difficult to conclude from numerical simulations of the ODE model (16) how large the delay effect is in real experiments. This question will the matter of future investigations.

8 Conclusion

In this work, we have presented a new framework for the functional identification of non-monotonic growth functions in the chemostat. Continuous and discrete time variants have been proposed. Numerical simulations illustrate the potential of the method. Further investigations are required to find out which approach (discrete or continous) is better suited for real experiments.

The approach is more general than the case we have presented here for the chemostat model. We introduce feedback control to reduce a dynamical system to an algebraic equation. Then we apply either numerical methods (in discrete time) or dynamical equations (in continuous time) to identify unstable equilibria of the original uncontrolled dynamical system. We use the chemostat as a conceptually simple example that is still of practical interest.

Another application we plan to explore in the future are regulation problems. For example, one can regulate the single-species chemostat to operate at the substrate concentration s at which the growth rate μ is maximal by following the same recipe. This approach to regulation, which is similar in spirit to the act-and-wait technique for delay compensation [15], does not require an a-priori identification of the growth rate μ, and leads to a different algorithm than the methods discussed in the literature [13, 14]).

References

[1] E. H. Abed, H. O. Wang and R. C. Chen, *Stabilization of period doubling bifurcations and implicatons for control of chaos*, Physica D, vol. 70, 1994, pp. 154–164.

[2] E. L. Allgower and K. Georg *Introduction to Numerical Continuation Methods*, Society for Industrial and Applied Mathematics, 2003.

[3] R. Antonelli, J. Harmand and J. P. Steyer and A. Astolfi. *Set point regulation of an anaerobic digestion process with bounded output feedback*, IEEE transactions on Control Systems Technology, vol. 11, 2003, pp. 495–504.

[4] G. Bastin and D. Dochain, *On-Line Estimation and Adaptive Control of Bioreactors*, Elsevier, Amsterdam, 1990.

[5] E. Benoît, *Dynamic bifurcations: proceedings of a conference held in Luminy, France, March 5-10, 1990*, Lecture Notes in Mathematics vol. **1493**, Springer-Verlag, 1991.

[6] H. Boudjellaba, T. Sari, *Stability Loss Delay in Harvesting Competing Populations*, J. Differential Equations, vol. 152, 1999, pp. 394–408.

[7] F. Campillo and C. Lobry, *Effect of population size in a Prey-Predator model*, preprint, 2011 `http://arxiv.org/abs/1111.6460`.

[8] D. Dochain *State and parameter estimation in chemical and biochemical processes : a survey.* Journal of Process Control, Vol. 13 (8), 2003, pp. 801–818.

[9] D. Dochain and G. Bastin. *Adaptive identification and control algorithms for non linear bacterial growth systems.* Automatica, vol 20 (5), 1984, pp. 621–634.

[10] D. Dochain and G. Bastin. *On-line estimation of microbial growth rates.* Automatica, Vol. 22 (6), 1986, pp. 705–711.

[11] D. Dochain and A. Pauss. *On-line estimation of specific growth rates : an illustrative case study.* Canadian Journal of Chemical Engineering, Vol. 66 (4), 1988, pp. 626–631.

[12] D. Dochain and M. Perrier. *Dynamical Modelling, Analysis, Monitoring and Control Design for Nonlinear Bioprocesses* Advances in Biochemical Engineering Biotechnology, vol. 56, 1997, pp. 147–197,

[13] D. Dochain, M. Perrier and M. Guay. *Extremum Seeking Control and its Application to Process and Reaction Systems: A Survey.* Mathematics and Computers in Simulation, Special Issue, to appear.

[14] M. Guay, D. Dochain and M. Perrier. *Adaptive extremum seeking control of stirred tank bioreactors.* Automatica, 40 (5), 2004, pp. 881–888.

[15] T. Insperger. *Act-and-wait concept for continuous-time control systems with feedback delay.* IEEE Transactions on Control Systems Technology, 14(5), 2006, pp. 974–977.

[16] M. Perrier, S. Feyo de Azevedo, E. Ferreira and D. Dochain. *Tuning of observer-based estimators: theory and application to the on-line estimation of kinetic parameters* Control Engineering Practice, vol. 8 (4), 2000, pp. 377–388.

[17] K. Pyragas, *Continuous control of chaos by self-controlling feedback*, Phys. Letters A, vol. 170, 1992, pp. 421–428.

[18] J. Sieber, A. Gonzalez-Buelga, S. A. Neild, D. J. Wagg and B. Krauskopf, *Experimental continuation of periodic orbits through a fold*, Phys. Rev. Lett., vol. 100, 2008, 244101.

[19] H. L. Smith and P. Waltman, *The Theory of the Chemostat*, Cambridge University Press, 1995.

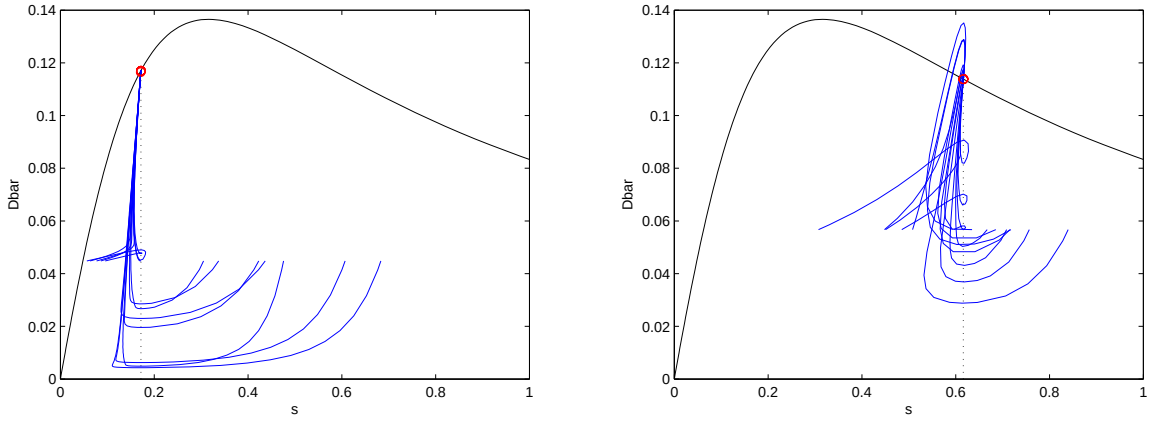

Figure 3: Simulations for two different values of $\bar{s}$ in the (s, D)-projection.

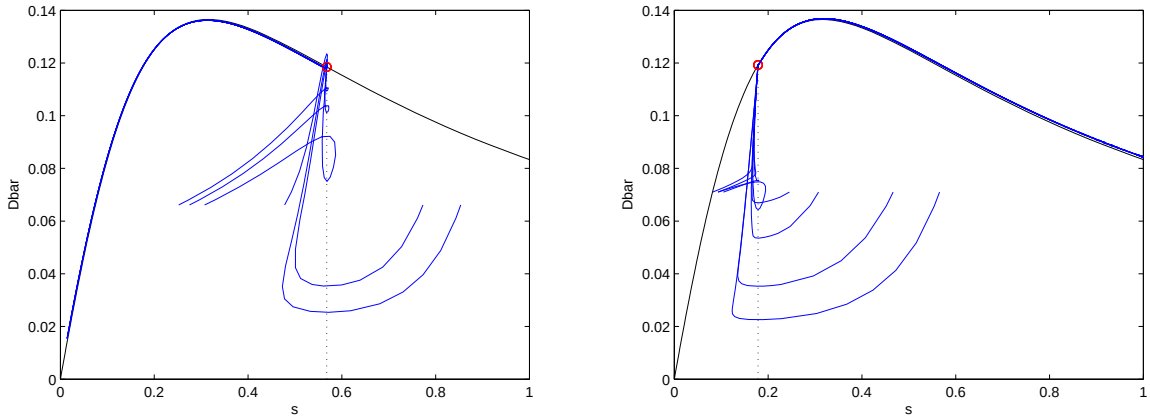

Figure 4: Dynamical continuation using (12) to explore dynamically the left and right part of the graph of the unknown function $\mu(\cdot)$.

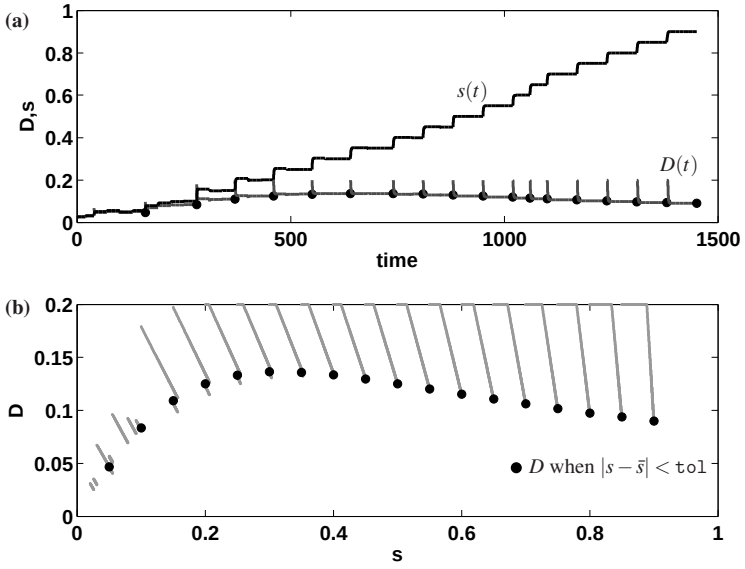

Figure 5: Simulation of discrete-time continuation using (13) where $\bar{s}_k = 0.05k$. Panel (a) shows the time profile of output s and input D throughout the run. Panel (b) shows the same in the (s, D)-plane. Black dots indicate when convergence ($|s_{\text{eq}} - \bar{s}_k| < \texttt{tol}$) was reached, and the iteration moved on to the next $\bar{s}_k$. Parameters: $\texttt{tol} = 10^{-4}$, $G_1 = 1/(s_{\text{in}} - \bar{s}_k)$, $D_{\max} = 0.2$, $D_{\min} = 0.02$. Transients were accepted as settled if $\max s - \min s < 0.1$ on the interval $[t - 10, t]$.

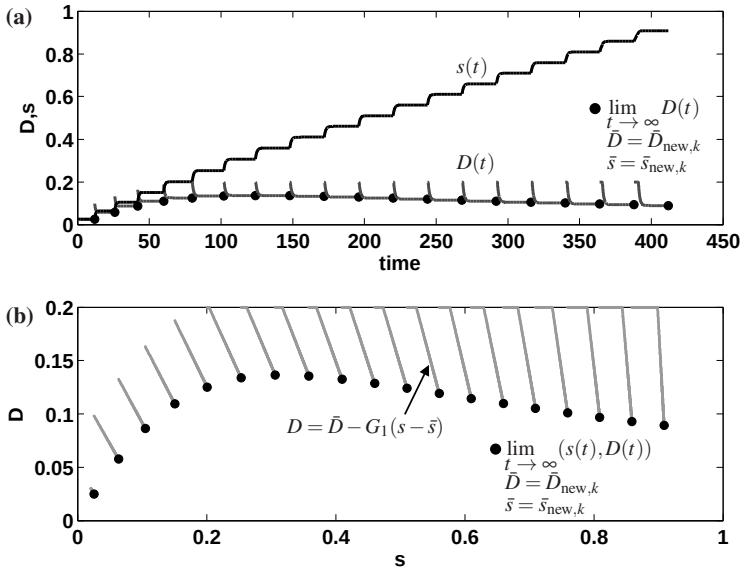

Figure 6: Simulation of simplified discrete-time continuation using (14)–(15) where $\delta = 0.05$. Note the shorter time scales on the x-axis of panel (a) compared to Figure 5. The convention in the panels and the parameters are identical to Figure 5.

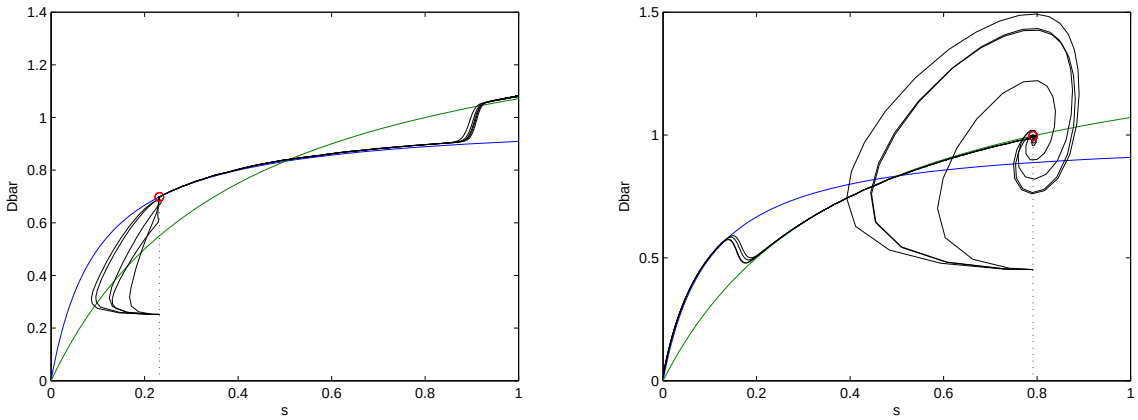

Figure 7: Stability loss delay in the continuation method for the two species case ($\bar{s}$ is increasing on the left figure, and decreasing on the right one)